available at www.sciencedirect.com

ScienceDirect

journal homepage: www.elsevier.com/locate/funeco

Phylogenetic, structural and functional diversification of nitrate transporters in three ecologically diverse clades of mushroom-forming fungi

Jason C. SLOT[a,b,*], *Kelly N. HALLSTROM*[a], *P. Brandon MATHENY*[c], *Kentaro HOSAKA*[d], *Gregory MUELLER*[e], *Deborah L. ROBERTSON*[a], *David S. HIBBETT*[a]

[a]*Department of Biology, Clark University, Worcester, MA, USA*
[b]*Department of Biological Sciences, Vanderbilt University, Nashville, TN, USA*
[c]*Department of Ecology & Evolutionary Biology, University of Tennessee, Knoxville, TN, USA*
[d]*Department of Botany, National Museum of Nature and Science, Japan*
[e]*Chicago Botanic Garden, USA*

ARTICLE INFO

Article history:
Received 22 April 2009
Revision received 24 August 2009
Accepted 14 September 2009
Available online 16 December 2009
Corresponding editor: Petr Baldrian

Keywords:
Coprinopsis
Coprinus
Hebeloma
Hydnangiaceae
Laccaria
Nitrate
NRT2
Psathyrellaceae
Selection
Transporter

ABSTRACT

Nrt2 encodes a transporter (NRT2) that facilitates nitrate assimilation in most lineages of Dikarya. We used degenerate PCR to examine *nrt2* sequence diversity and phylogeny in three clades of mushroom-forming basidiomycetes (*Hebeloma*, Hydnangiaceae and Psathyrellaceae) and tested for positive selection on *nrt2* in each lineage. We investigated the relative expression of *nrt2* paralogs in *Hebeloma helodes* and compared the patterns of expression between three *Hebeloma* and one *Gymnopilus* species, with quantitative PCR. Four lines of evidence of functional diversification in the nitrate assimilation system in mushroom-forming fungi emerged: (1) paralogs of *nrt2* were recovered in *Hebeloma* and Hydnangiaceae, but distribution was not complete; (2) two paralogs in *H. helodes* appear to be differently expressed; (3) structural differences in NRT2 are apparent between paralogs and lineages; and (4) *nrt2* is under significant positive selection in each lineage, and at least 6 sites are identified as under positive selection in the ectomycorrhizal family, Hydnangiaceae.

Introduction

Nitrate is a source of nitrogen that is subject to broad and rapid fluctuations in natural environments (Unkles *et al.* 2001). *Nrt2* encodes a high affinity nitrate transporter in the major facilitator superfamily (MFS) that facilitates nitrate assimilation in several eukaryotic lineages, including fungi. Members of the *nrt2* gene family encode transporters that vary by lineage and paralog in their affinity for nitrate (Zhou *et al.* 2000; Unkles *et al.* 2001). *Nrt2* appears to have been acquired by fungi

* *Corresponding author*. Department of Biological Sciences, Vanderbilt University, VU Station B #351634, Nashville, TN 37235, USA. Tel.: +1 615 936 3893.
E-mail address: jason.c.slot@vanderbilt.edu (J.C. Slot).
1754-5048/$ – see front matter
doi:10.1016/j.funeco.2009.10.001

as a coordinately regulated (Johnstone *et al.* 1990; Brito *et al.* 1996; Jargeat *et al.* 2003), three gene cluster. The acquisition likely occurred in Dikarya (Ascomycota and Basidiomycota) after its divergence from other fungal lineages, and it has subsequently been lost in some lineages (Slot & Hibbett 2007). To date, *nrt2* is the only characterized gene for nitrate transport in fungi.

Fungal *nrt2* is characterized by 12 transmembrane domains, MFS and nitrate/nitrite porter family (NNP) signature motifs, a short C-terminus and a large hydrophilic intracellular loop (IL) between the sixth and seventh transmembrane helices (Jargeat *et al.* 2003). The best characterized fungal NRT2 proteins are in *Aspergillus nidulans* (Unkles *et al.* 1991), *Hansenula polymorpha* (Brito *et al.* 1996) and *Tuber borchii* (Montanini *et al.* 2006) (ascomycetes), and *Hebeloma cylindrosporum* (Jargeat *et al.* 2003) (basidiomycetes). These have been shown to have substrate K_m values up to 100 μM NO_3 (unknown in *Hebeloma*), which is in the high affinity range. Their expression is induced by N-starvation and nitrate, and repressed by ammonium. The arginine residues in the *A. nidulans* NRTA (an NRT2 homolog) positions 87 and 368 (R87, R368) are universally present in other fungi and mutation analyses suggest R87 is essential to binding or transport of the substrate (Unkles *et al.* 2004). A putative protein kinase C (PKC) binding motif (S/T-x-R/K) at the N-terminal end of the large intracellular loop has been reported that distinguishes fungal from plant NRT2 proteins (Jargeat *et al.* 2003).

Three of the well-characterized fungal *nrt2* genes are likely or confirmed single-copy genes. *A. nidulans* possesses two functionally distinct isoforms (Unkles *et al.* 2001). Diversification of the *nrt2* family (in general) is widespread, with plants apparently possessing the largest number of paralogs present at one time in an individual species (Orsel *et al.* 2002). Oomycetes (heterokonts) also possess multiple copies of *nrt2* (Slot *et al.* 2007). Fungi, however, with more than sixty genomes sequenced, have not been shown to possess more than two copies, usually having only a single gene copy (Slot *et al.* 2007).

The two NRT2 isoforms in *A. nidulans*, NRTA and NRTB, are functionally distinct, having K_m values of 100 μM and 10 μM respectively, but appear to be under identical transcriptional regulation (Unkles *et al.* 2001). NRTA may be under post-translational regulation (Wang *et al.* 2007), which could mean further functional divergence between these isoforms.

In this study we have analyzed the patterns of diversification of *nrt2* in three lineages of mushroom-forming basidiomycetes with different ecological niches. *Hebeloma* and Hydnangiaceae are two lineages of ectomycorrhizal symbionts of plants, while Psathyrellaceae is a family mostly composed of wood and dung decomposing saprotrophs. The niches within these lineages are highly varied with respect to nitrogen form and availability. *Hebeloma*, for instance, contains sand-loving (*H. cylindrosporum*, *Hebeloma affine*) species, animal latrine associates (e.g. *Hebeloma radicosum*), and carcass associates (*Hebeloma syrjense*), in addition to taxa with apparently less extreme niches (*Hebeloma velutipes* and *Hebeloma helodes*, which are widespread mycorrhizal fungi without clearly defined nitrogen preferences). We, therefore, expected to find structural differences among *nrt2* in fungi from such a variety of niches, and amino acid sites that are under positive selection, which could suggest functional adaptation. We further expected that each of the divergent *nrt2* paralogs previously discovered (Slot *et al.* 2007) in *H. helodes* (*Hhnrt2.1* and *Hhnrt2.2*) would be expressed in a specific range of nitrate concentrations, suggestive of sub-functionalization, and that relative expression of *nrt2* orthologs in related species would reflect niche divergence with regards to nitrogen availability. Finally, we examined *nrt2* sequences from seven complete *Aspergillus* genomes, to provide a more complete context for comparisons between isoforms investigated here and those previously characterized in *Aspergillus*, and to investigate the pattern of gene clustering of *nrt2* paralogs in a model system.

Materials and methods

Specimens and cultures

Basidiocarps (Table 1) were collected and immediately dehydrated under moving air and mild heating to preserve DNA. Dikaryotic cultures, obtained *de novo* or from existing cultures from basidiocarps, were maintained on either Malt Extract Agar or Corn Meal Agar in ambient light at room temperature.

Molecular methods

DNA was extracted as described previously (Slot *et al.* 2007) or with DNeasy™ Plant DNA Extraction Kit (Qiagen, Valencia, CA, USA) according to the manufacturer's instructions. *Nrt2* was amplified by PCR using degenerate primers described in Slot *et al.* (2007). Internal transcribed spacers 1&2 (ITS) of the ribosomal RNA tandem repeat DNA were amplified using fungus specific primers (Gardes & Bruns 1993). Table 1 details longest *nrt2* amplicons obtained for each species in this study. All *nrt2* products were ligated into cloning vectors to transform chemically competent Top10 or DH5-α *Escherichia coli* with the TA cloning kit version V or Topo TA cloning kit version R (Invitrogen, Carlsbad, CA, USA). Many ITS products were also cloned due to length heterogeneity.

Full-length coding sequences were obtained for *H. helodes* *nrt2* copy 1 (*Hhnrt2.1*) and copy 2 (*Hhnrt2.2*) with the following procedure: RNA was extracted using the Rneasy Plant Minikit (Qiagen, Valencia, CA, USA). 5′ sequence was obtained with the 5′ RACE System for Rapid Amplification of cDNA Ends, Version 2.0 (Invitrogen, Carlsbad, CA, USA) using a gene specific primer targeted to the rapidly evolving large intracellular loop for first strand synthesis of cDNA and a nested gene specific primer within 600 bp of the start codon for PCR. PCR products of expected size were excised from a 1.2 % agarose gel electrophoresed in TBE (1X). Products were cloned as above. 3′ sequence was obtained using an adapter primer targeted to the poly-A tail of mRNA for first strand cDNA synthesis, followed by PCR with a universal amplification primer (UAP) and gene specific primers within 800 bp of the stop codon. PCR with nested gene specific primers and UAP yielded a single band that was cloned as above. Assembly of sequences of multiple PCR products was used to design specific primers for the full-length sequence of each paralog, and products were obtained and sequenced from genomic DNA.

Table 1 – Strains used in this study

Species	Sources of materials and cultures	Amplification primers	ITS accession	*Nrt2* accession	ID[a,b]
Agrocybe erebia	Worcester, MA	f2/r2.6	FJ168567	FJ168612	JCS101405
Coprinellus curtus	Hilo, HI	f2/r2.6	AY461834	FJ168613	DEH630
Coprinellus disseminatus	Hilo, HI	f2/r2.6	AY461838	FJ168614	MRK18
Coprinellus micaceus	S. Grafton, MA	f2/r2.6	FJ168568	FJ168615	JCS042505
Coprinellus radians	Pu'u La'au, HI	f2/r2.6	AY461815	FJ168616	DEH1026
Coprinellus radians	Hilo, HI	f2/r2.6	AY461818	FJ168617	DEH1765
Coprinopsis atramentaria	King County, WA	f2/r2.6	FJ168570	FJ168618	PBM992 (WTU)
Coprinopsis cinerea	Hilo, HI	f2/r2.6	AY461825	FJ168619	DEH2065
Coprinus sp.	S. Grafton, MA	f2/r2.6	FJ168570	FJ168620	JCS101305
Gymnopilus junonius	S.Grafton, MA	f1/r3	FJ168571	EF520283	JCS102604A +C[c]
Hebeloma affine	Ontario, Canada	f2/r2.6	FJ436320	FJ168621, FJ168622	NI270904
H. cylindrosporum	Hulshorst, Netherlands	f1/hr2	FJ168572	EF520278	CBS557.96 =C[d]
H. cylindrosporum	Hulshorst, Netherlands	f1/r3	FJ168573	EF520276	CBS558.96 =C
H. edurum	France	f1/hr2	FJ168574	EF520259	CBS291.50 =C
H. helodes	Rhinebeck, NY	f3/r3	FJ168575	EF520265	JCS102604C
H. helodes	Rhinebeck, NY	Full length	FJ168576	FJ168623, FJ168624	JCS92306A +C
H. helodes	Worcester, MA	f1/r3, f1,hr2	FJ168577	EF520270, EF520268	PBM2687
H. helodes	Keystone, CO	f1/hr2, f2/r2.6	FJ168578	FJ168625, FJ168626	PBM2712
H. helodes	Rhinebeck, NY	f2/r2.6	FJ168579	FJ168627	JCS102604B
H. mesophaeum	Keystone, CO	f1/r2.6	FJ168580	FJ168628, FJ168629	PBM2734
H. radicosum	France	f1/hr2	FJ168581	EF520275	CBS183.47 =C
H. radicosum	Japan	f2/r2.6	FJ168582	FJ168630	MYA2661 =C
H. sinuosum	France	f1/hr2	FJ168584	EF520260	CBS184.47 =C
H. tomentosum group	Rutland, MA	f3/r3	FJ168583	EF520261	PBM2693
H. tomentosum group	Uxbridge, MA	f2/r2.6	FJ168586	FJ168632	JCS101905C
H. tomentosum group	S. Grafton, MA	f1/hr2	FJ168587	EF520263	JCS91904A
H. truncatum	France	f3/r3	FJ168588	EF520272	CBS295.50 =C
H. velutipes	Lincoln, MA	f2/r2.6	FJ168589	FJ168633	JCS100905H
H. velutipes	Sutton, MA	f2/r2.6	FJ168590	FJ168634	JCS101105A
H. velutipes	S. Grafton, MA	f2/r2.6	FJ168591	FJ168635	JCS102305A
H. velutipes	S. Grafton, MA	f2/r2.6	FJ168592	FJ168636	JCS91706A +C
H. velutipes	S. Grafton, MA	f2/r2.6	FJ168593	FJ168637	JCS100905K
Hebeloma velutipes	Lincoln, MA	f2/r2.6	FJ168585	FJ168631	PBM2674
Hebeloma sp.	France	f1/hr2	FJ168594	EF520271	CBS163.46
Hydnangium carneum	Australia	f2/r2.6	FJ168599	FJ168643, FJ168644	GMM7271
Hydnangium sp.	New Zealand	f2/r2.6	FJ168595	FJ168638, FJ168639	KHNZ06123
Laccaria lateritia	Australia	f2/r2.6	FJ168596	FJ168640	GMM7243
L. ochropurpurea	Rhinebeck, NY	f2/r2.6	FJ168600	FJ168645, FJ168646	JCS091506
Laccaria sp.	Thailand	f2/r2.6	FJ168597	FJ168641, FJ168642	DED7419
Laccaria sp.	Douglas, MA	f2/r2.6	FJ168598	EF520279, EF520280	SK05030
Laccaria sp.	Douglas, MA	f2/r2.6	FJ168601	FJ168647	SK05031
Laccaria sp.	Sutton, MA	f2/r2.6	FJ168602	FJ168648, FJ168649	JCS071005C
Laccaria sp.	MS	f2/r2.6	FJ168603	FJ168650	GMM1080
Laccaria sp.	Douglas, MA	f2/r2.6	FJ168604	EF520281, EF520282	SK05034
Laccaria sp.	S. Grafton, MA	f2/r2.6	FJ168605	FJ168651, FJ168652	JCS071205
Laccaria sp.	Australia	f2/r2.6	FJ168606	FJ168653, FJ168654	GMM7238
Psathyrella candolleana	S. Grafton, MA	f2/r2.6	FJ168607	FJ168655	JCS070705
Psathyrella hymenocephala	Worcester, MA	f2/r2.6	FJ168608	FJ168656	PBM2766
Psathyrella hymenocephala	Worcester, MA	f2/r2.6	FJ168609	FJ168657	PBM2768
Psathyrella spadicea	S. Grafton, MA	f2/r2.6	FJ168610	FJ168658	JCS100905B

a Location of collections, unless otherwise noted: Prefixes JCS, SK = Clark University Fungal Herbarium, PBM = TENN (Brandon Matheny), GMM, KH, DED = FMNH, DEH, MRK = SFSU, NI = TENN, DAOM (Nancy Ironside).
b Curation of cultures: Prefix CBS = Centraalbureau voor Schimmelcultures, MYA = ATCC, JCS = Jason Slot, personal culture/collection.
c Culture and collection.
d Culture only.

PCR products were sequenced using BigDye v3.1 (Applied Biosystems (ABI), Foster City, CA, USA) and analyzed on an ABI 3130 or 3730 genetic analyzer. Multiple primer extension sequences were assembled to ensure double-stranded coverage using Sequencher 4.7 (Gene Codes Corporation, Ann Arbor, MI).

Phylogenetic analyses: alignment

ITS sequences for all specimens used in this study were assembled into either a pre-existing matrix (Aanen *et al.* 2000), for *Hebeloma*, or matrices assembled *de novo* with reference to previous analyses in Psathyrellaceae (Padamsee *et al.* 2008) and

Laccaria (Hydnangiaceae) (Osmundson *et al.* 2005). Sequences were aligned with MAFFT v. 6.525 (Katoh & Toh 2008) and adjusted manually (Table 2). Relationships between the present samples and previously studied strains were estimated with neighbor joining analyses using Kimura-2 distances (Supplementary material Figs S1–3) in PAUP*4.0b (Swofford 2003).

Matrices of ITS and *nrt2* nucleotides were assembled manually, and with reference to previous work (Slot *et al.* 2007) in MacClade 4.08 (Maddison & Maddison 2000). Exon matrices of *nrt2* were assembled that included all taxa in the study, and separate matrices of *nrt2* and ITS of individual subgroups were assembled using *Gymnopilus* or *Agrocybe* as outgroups. Hydnangiaceae and *Hebeloma* matrices contained intron and exon sequences, and the Psathyrellaceae matrix contained exon sequence only as introns were not alignable. For comparison with completely sequenced genomes, an alignment using *nrt2* exon sequences from seven complete *Aspergillus* genomes was also analyzed.

Phylogenetic anaylyses: approaches

Alignments were subjected to Bayesian inference (with MrBayes ver. 3.1.2p (Ronquist & Huelsenbeck 2003; Altekar *et al.* 2004)), maximum parsimony (in PAUP*4.0b (Swofford 2003)) and maximum likelihood (ML) (in RAxML 7.0.3 (Stamatakis 2006)) analyses. Datasets were partitioned by codon position (and non-coding sequence where applicable) in Bayesian and ML analyses. Bayesian analyses were performed under a GTR plus gamma nucleotide substitution model for one million generations and the trees generated before likelihoods of two parallel chains converged were removed as the burnin. RAxML analyses were performed under the GTRMIX model. One thousand RAxML bootstrap replicates were performed with the –f a algorithm, and –f b and –f d algorithms with slower hill climbing were also run for comparison. 1 000 bootstrap replicates were performed for maximum parsimony analyses, using TBR and saving 100 trees per addition sequence replicate.

Phylogenetic analyses: hypothesis testing

A constrained analysis was performed in RaxML that forced the primary paralog of *nrt2* to be monophyletic in *Hebeloma*, using *Gymnopilus junonius* as an outgroup. A second constrained analysis was performed forcing the monophyly of *Coprinellus* and section Candolleana in the Psathyrellaceae dataset using *Agrocybe erebia* as an outgroup. A Shimodaira–Hasegawa (SH) test, implemented in RaxML, was used to test for significant differences between likelihoods of alternative topologies.

A test of selection was performed on each independent *nrt2* alignment with the Selecton ver. 2.4 (Doron-Faigenboim *et al.* 2005; Stern *et al.* 2007) online server (http://selecton.tau.ac.il/index.html) using the ML topology for ancestral state reconstruction. The Mechanical Empirical Combination Model (MEC) (Doron-Faigenboim & Pupko 2007) was chosen, using a JTT amino acid matrix and eight or 20 distribution categories at intermediate precision. This method calculates an empirical Bayesian estimation and posterior probability of the ratio of non-synonymous to synonymous substitution (K_a/K_s) for each amino acid site in the alignment, using a ML topology naïve to branch lengths. The estimation is calculated using an empirical amino acid substitution model that has been converted into a codon substitution probability matrix in which each substitution is weighted according to theoretical codon frequencies and nucleotide transition–transversion bias. The Akaike Information Content (AIC) scores of the MEC and an M8a null model, which did not allow K_a/K_s to be greater than 1, were compared in Selecton to test for significance (Table 2). The M5, gamma (M5) and M8, beta + $\omega \geq 1$ (M8) models, which do not account for an amino acid substitution matrix were also tested on the Hydnangiaceae alignment, and the significance of the M8 was evaluated by a likelihood ratio test *versus* the M8a null model.

Sequence structure analyses

NRT2 primary structure was inferred by excision of putative introns as described previously (Slot *et al.* 2007) and translation in batches using the RevTrans 1.4 server (http://www.cbs.dtu.dk/services/RevTrans/). We performed helical wheel analysis on a selection of inferred amino acid sequences using the Java applet at the Interactive Biochemistry site, http://cti.itc.virginia.edu/~cmg/ (created by Edward K. O'Neil and Charles M. Grisham at the University of Virginia in Charlottesville). We analyzed the C-terminal portions of the second transmembrane motif around a universally conserved arginine

Table 2 – Description of alignments for phylogenetic analyses

Alignment	Phylogenetic analysis – most inclusive dataset					Selection – codons only		
	Terminals	Length (codon)	PIC[a]	MPD[b]	Tree length[c]	MEC L[d]	M8a L[e]	AIC dif[f]
Hebeloma	31	2 173 (1 578)	815	719	1 676.90768	−7 596.4	−7 628.19	61.568
Hydnangium	16	994 (795)	377	316	1 226.82335	−4 357.65	−4 423.8	130.274
Psathyrella	14	(795)	425	343	1 115.93295	−4 879.99	−4 976.37	190.735
Aspergillus	12	(1 557)	770	634	2 173.12596	−11 047.8	−11 235.3	372.987

a PIC = number of characters inferred to be parsimony informative.
b Maximum phylogenetic distance, estimated by absolute character difference matrix.
c The sum of total character differences in the maximum likelihood topology.
d The likelihood score of the MECjtt Selecton run.
e The likelihood score of the M8a Selecton run which assumes a neutral model of selection.
f The difference between Aikake Information Content scores (AIC) of MECjtt and M8a models.

Table 3 – Real time RT-PCR expression species

Species and transcript	Strain ID	Amplicon size (bp)	Forward primer	Reverse primer
H. helodes				
paralog 1	JCS92306A	149	cct ggc gag cag ctt tc	ggt gtc ctt gtt tga tgg caa gt
paralog 2		146	cat ggc gag cag cgt ttg	ccc cat ctc tgt ggg caa tc
ef1-α		163	tgg tcg tgt tga gac tgg tat ca	tcc ttg aca gac acg ttc ttg ac
H. radicosum				
nrt2	MYA2661	152	gcg agc agc gtt cac aat c	ggg ata tca tgc cct tgt ttg ac
ef1-α		169	Same as JCS92306A	cgg ata tct ttg aca gac acg ttc tta ac
H. velutipes				
nrt2	JCS91707A	139	gag cag cct tcg caa tcg t	ccc ttg ttt tgc ggc gag
ef1-α		163	Same as JCS92306A	Same as JCS92306A
G. spectabilis				
nrt2	JCS102604A	155	ctg gag agc ttc ttt tgc tgt tgt	cgt act tgg tgt cct tgc tga atg
ef1-α		163	Same as JCS92306A	tcc ttg acg gag acg ttc ttg ac

residue (R87) and on 18 residues in the sixth and twelfth transmembrane motifs. The arginine residues, R87 and R368 were located through an amino acid alignment containing *A. nidulans* NRTA. Protein kinase C binding motifs (S/T-x-R/K) were calculated across an amino acid alignment with a Visual Basic Application written for that purpose by C. Khatchikian (Clark University), implemented in Microsoft Excel. The PESTfind algorithm (Rogers *et al.* 1986; Rechsteiner & Rogers 1996) was also used to search for potential post-translational modification motifs. A theoretical three-dimensional structure of *H. cylindrosporum* NRT2 (ModBase #Q9UVH7) was merged with positive selection data for the Hydnangiaceae alignment in Selecton and the model was annotated in Polyview-3D (Porollo *et al.* 2004; Porollo & Meller 2007).

Relative expression analyses

Dikaryotic mycelia for real time PCR were cultured under ambient conditions in a modified liquid N2P3 medium (12.6 mM glucose, 0.45 mM $CaCl_2 \cdot 2H_2O$, 0.61 mM $MgSO_4 \cdot 7H_2O$, 3.66 mM KH_2PO_4, 4.86 mM $Na_2HPO_4 \cdot 7H_2O$, 16.86 mM NaH_2PO_4, 0.048 mM ferric citrate, 120 nM thiamine, 1.6 nM D-biotin and 0.1 % f/2 micronutrients) containing 1.89 mM $(NH_4)_2SO_4$ as a sole nitrogen source. Media and nitrogen concentrations were chosen based on previous expression studies (Jargeat *et al.* 2003), which found that *nrt2* was not expressed in a dikaryotic strain of *H. cylindrosporum* after 12 d on 3.78 mM ammonium, and maximal *nrt2* expression was at 24 h. *Hebeloma* and *Gymnopilus* strains were sub-cultured into liquid N2P3 with ammonium as a sole nitrogen source for up to 12 d. When cultures were near confluence (estimated >75 % of the Petri dish area), fluid was removed by aspiration and exchanged by pipette three times for media with one of four concentrations (0, 3.78, 12.6, 25.2 mM) of nitrate-N ($NaNO_3$), 3.78 mM ammonium-N $(NH_4)_2SO_4$, or 3.78 mM ammonium nitrate-N (NH_4NO_3) as a sole nitrogen source for 24 h. RNA was extracted from three combined cultures using the Rneasy™ Plant minikit (Qiagen, Valencia, CA, USA) according to manufacturer's instructions. RNA was treated with gDNA wipeout buffer (Qiagen proprietary reagent for eliminating genomic DNA contamination) at 42 °C for 7 min. The treated RNA was diluted to 50 ng μl^{-1} according to optical density determined spectrophotometrically. Real time RT-PCR was performed in triplicate on a Stratagene Mx3000P™ thermal cycler with 50 ng of each dilution using the Quantifast™ SYBR® Green RT-PCR kit (Qiagen, Valencia, CA, USA). All real time PCR experiments were followed by dissociation curve analysis. Amplicons from each primer pair (Table 3) were examined on an agarose gel to verify amplicon size, to confirm processing and assure that multiple products were not generated. Raw fluorescence data were used to determine amplification efficiency for individual replicates using the SimFit module (Batsch *et al.* 2008) in Pro-Fit 6.1.8 (QuantumSoft). Theoretical initial template (R_o) was calculated by first deriving the average efficiencies of replicate PCR reactions using the following equation:

$$F_x = F_0 \cdot (EA)^x$$

where the amplification efficiency (EA) and theoretical initial fluorescence (F_0) are estimated by an iterative Gaussian curve-fitting algorithm that best models observed fluorescence (F) at cycle x. EA was then used to calculate the theoretical initial template (assuming product to be proportional to fluorescence) when:

$$Ro = EA^{-Ct}$$

and Ct (the cycle threshold) is calculated by MXPro Mx3000P™ ver. 3.0 software (Stratagene, La Jolla, CA, USA). Expression levels relative to the housekeeping gene *ef1-α* were then calculated as a simple ratio. Results were independently verified with Dart PCR (Peirson *et al.* 2003), which calculates EA by log-linear regression of ROX-normalized fluorescence. Results were plotted with Pro-Fit.

Results

Degenerate PCR

Multiple clones (usually 5–10) of *nrt2* PCR products were generated from Psathyrellaceae (13 collections), *Hebeloma* (9 cultures, 15 collections), Hydnangiaceae (12 collections), *G. junonius* (1 culture) and *A. erebia* (1 collection) (Table 1). Most sequences were 900–1 800 bp in length, and all included the IL. Where paralogs were found, individual primer pairs favored amplification of one or the other paralog in *Hebeloma*, except in collection PBM2734 *Hebeloma mesophaeum*. Approximate amplicon

lengths for each primer pair were as follows: f2/r2.6 ~ 1 000 bp, f1/r3 ~ 1 900 bp, f3/r3 ~ 1 200 bp and f1/hr2 ~ 1 600 bp.

Full-length gene sequencing

Amplicons of the coding sequence of each paralog in *H. helodes* were assembled with the corresponding 5′ and 3′ RACE sequence to obtain the complete sequence (Fig 1). 2 091 bp of *Hhnrt2.1* were retrieved, of which 1 572 were coding and 585 intron, and 2 253 bp of *Hhnrt2.2* of which 1 563 were coding and 603 intron. The difference in coding length corresponded to three amino acids in the IL. For *Hhnrt2.1*, 27 nucleotides of the 5′ untranscribed region (UTR, incomplete) and 42 nucleotides of 3′ UTR (not including poly-A tail) were sequenced. For the second paralog, 123 nucleotides of 5′ UTR and 112 nucleotides of 3′ UTR (not including poly-A tail) were sequenced. Intron positions 1, 2, and 7 were confirmed in the process of obtaining RACE sequence. Intron position 4 was confirmed in the process of relative expression analyses. Start positions were inferred by similarity with published *H. cylindrosporum nrt2* (CAB60009) and were the first ATG codon in the 5′ RACE sequences.

Phylogenetic analyses

Phylogenetic relationships inferred with ITS (Fig 2) were mostly congruent with those inferred with *nrt2* (Figs 3, 4). Support for conflict between the two gene phylogenies is limited to a single node in Psathyrellaceae. The *nrt2* alignment, which was a longer matrix both with codons (Fig 3) and genomic sequence (Fig 4, *Hebeloma* and Hydnangiaceae), produced more resolved phylogenies than ITS using the same methods for identical taxon samples (*nrt2* alignments contain allelic and paralogous sequences). Two of the strongly supported nodes in the *nrt2* analyses represent gene duplications.

Specific nodes that received significant support from each gene are in Table 4. *Hebeloma*, Hydnangiaceae and Psathyrellaceae were all strongly supported as monophyletic in our datasets. In the codon dataset (Fig 4), *nrt2* weakly supported a paraphyletic *Hydnangium* (.98 BPP, 73MPB, 60MLB), suggesting either multiple origins or, less likely, reversal of the gasteroid (enclosed reproductive surface) state in this lineage. In the restricted Psathyrellaceae datasets (Figs 2, 4), there was an apparent conflict concerning the *Coprinellus/Candolleana* clade (node 13). ITS supported a published arrangement (Padamsee *et al.* 2008), but *nrt2* supported a more complex assemblage of *Coprinopsis*, *Psathyrella spadicea* and *Candolleana* (node 14). An SH test found no significant differences between the two topologies using the restricted *nrt2* codon alignment. The discovery of an *nrt2* sequence in *A. erebia* is the first molecular evidence for nitrate assimilation in the clade that possibly contains Inocybaceae, Crepidotaceae, Tubarieae and Panaeoleae (Matheny *et al.* 2006).

Gene duplication

The *nrt2* phylogenies (Fig 4) suggest an early duplication in *Hebeloma* and a recent duplication in *Laccaria* sp. DED7419. Inferred intrageneric paralogs in *Hebeloma*, *Laccaria* and

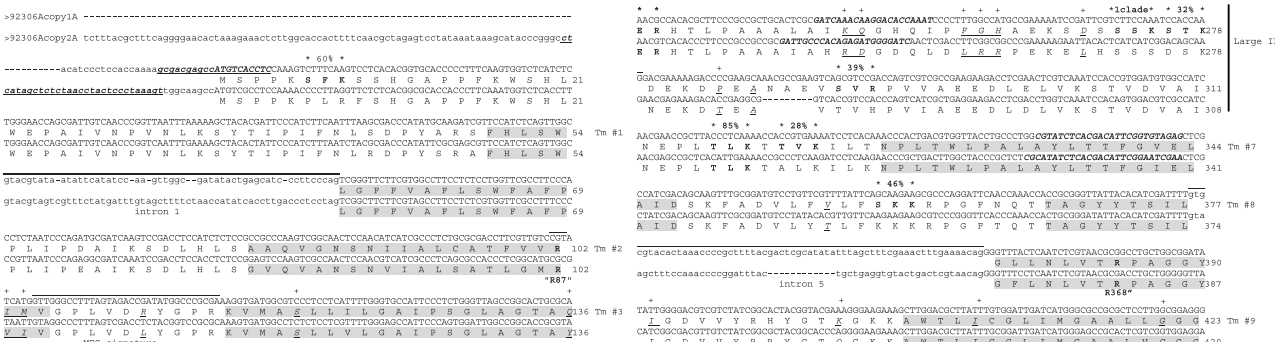

Fig 1 – Complete coding sequences and translations of *nrt2* paralogs in *H. helodes*. Primer sites for genomic DNA PCR are bold, italic underlined nucleotides, and primer sites for RACE PCR are bold, italic nucleotides. Transmembrane motifs are highlighted and labeled to the right according to previous work (Jargeat *et al.* 2003; Slot *et al.* 2007). Potential protein kinase C (PKC) motifs are bold in the amino acid translation and percentage of sequences presenting them in the combined dataset is noted between asterisks. The percentage of PKC conservation at AA position # 6 represents only five sequences. Highly conserved arginine residues are overlined, bold and labeled R87 and R368. Other conserved sites are overlined and labeled below. Sites with $K_a/K_s > 1$ are underlined, italic with "+" above. Introns are as in previous work (Slot *et al.* 2007).

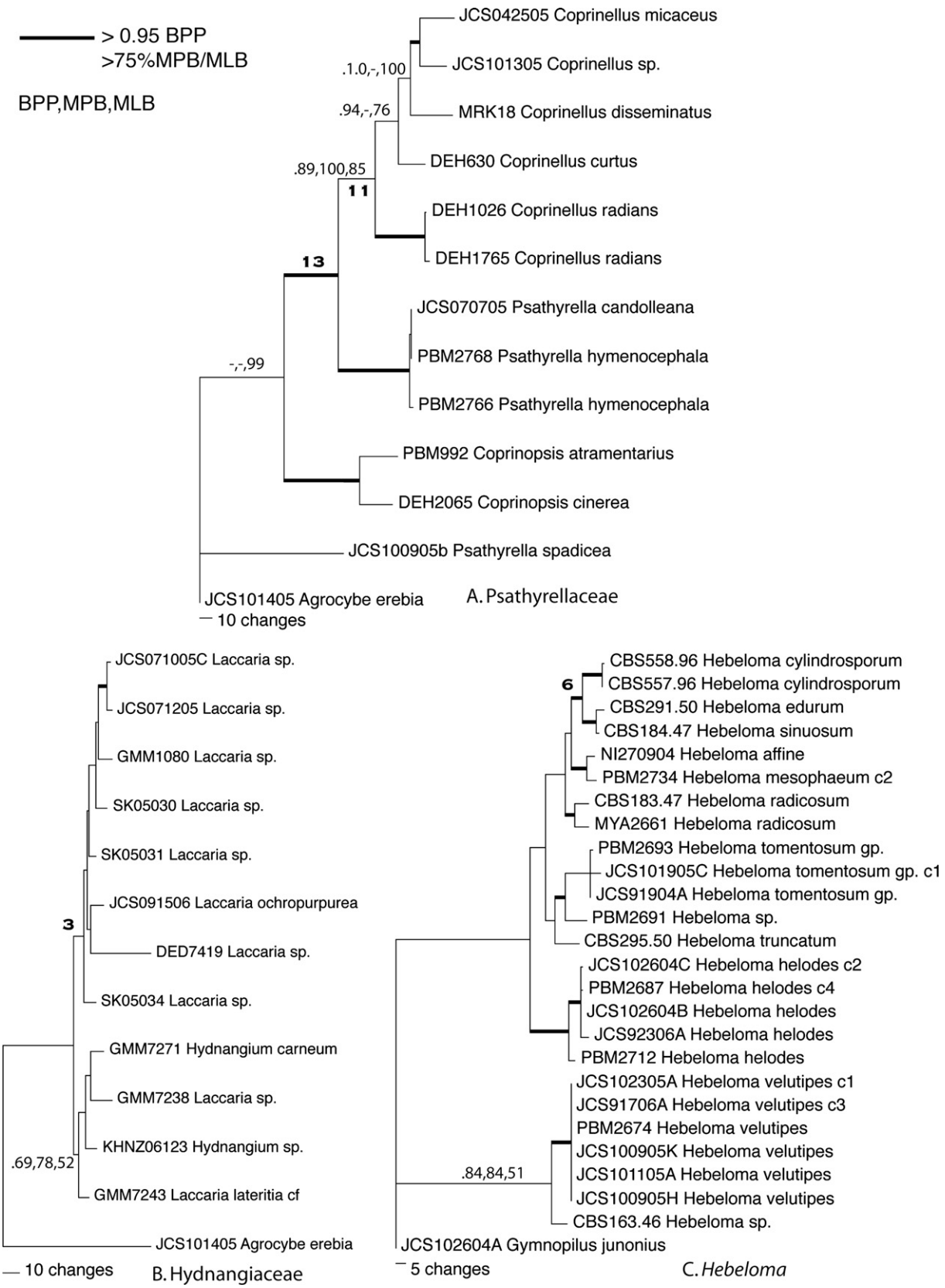

Fig 2 – Phylogenetic analyses of ITS in isolated genera. RAxML topology optimized with maximum parsimony. Outgroups were chosen from the initial broad analysis (Fig 3). Supported nodes are as in Fig 2. Supported nodes are indicated as follows: thickened black branches indicate greater than .95 Bayesian Posterior Probabilities (BPP) and greater than 75 % of Maximum Parsimony (MPB) and Maximum Likelihood Bootstrap (MLB) replicates. Thickened grey branches indicate greater than .90 BPP and greater than 60 % MPB and MLB. Subset support is noted for nodes close to these levels of significance. Nodes numbered in bold are as in Table 4. c1, c2, etc. represent sequences isolated by cloning from mixed PCR products.

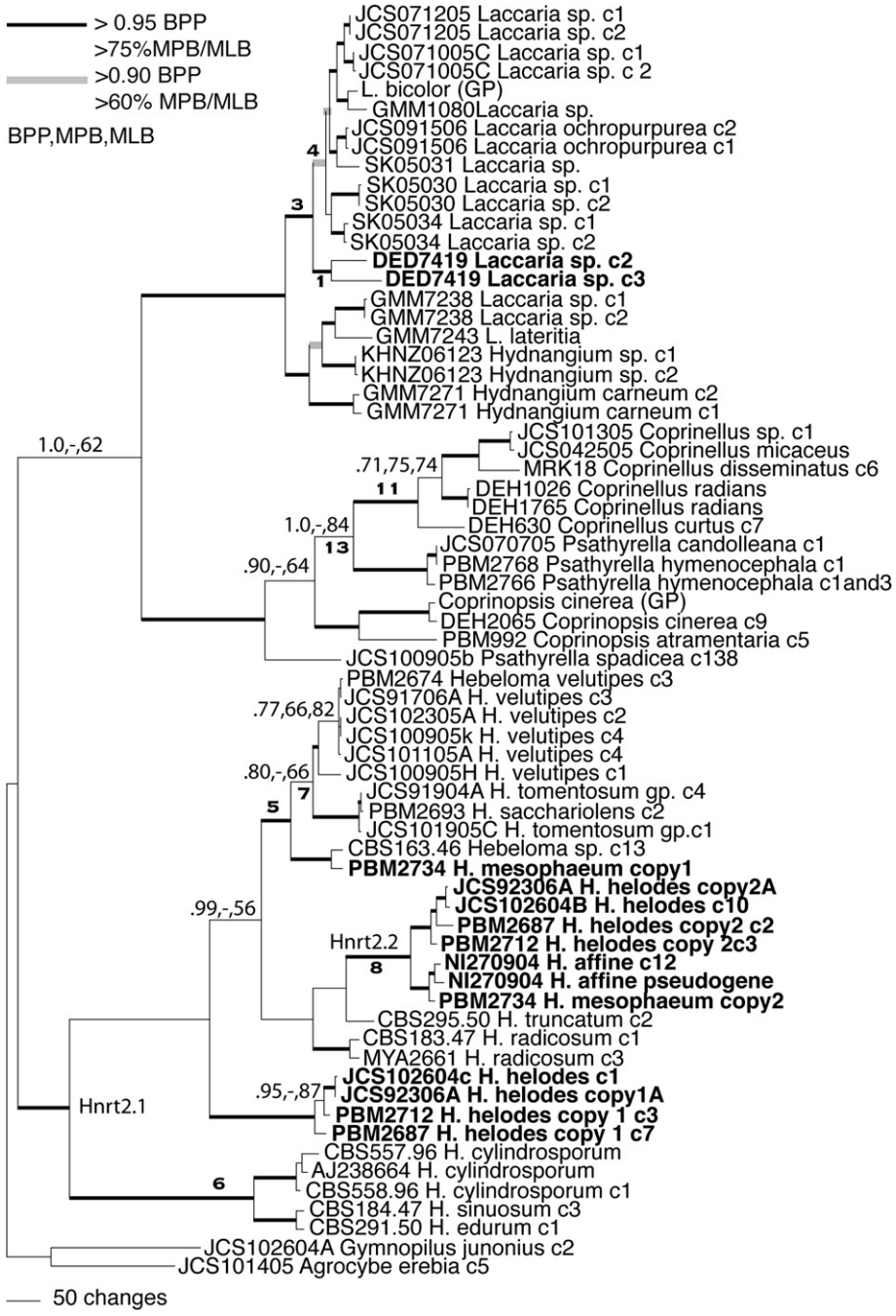

Fig 3 – Phylogenetic analysis of *nrt2* codon sequences generated in this study. Presented as in Fig 2. Sequences noted with (GP) indicate that they were obtained from complete genome projects of *Laccaria bicolor* (http://genome.jgi-psf.org/Lacbi1/Lacbi1.home.html) and *Coprinopsis cinerea* (http://www.broad.mit.edu/annotation/genome/coprinus_cinereus/Home.html). Sequences in bold are paralogous in taxa that contain them. The sequence AJ238664 was generated in previous work (Jargeat *et al.* 2003). Supported nodes are as in Fig 2. Nodes numbered in bold are as in Table 4. c1, c2, etc. is as in Fig 2.

Aspergillus were monophyletic, except complete data analyses within *Hebeloma* support *Hnrt2.2* nested within *Hnrt2.1* (1.0 BPP, 79 MPB, 53MLB). An SH test found no significant difference between the likelihood of the optimal tree and the tree forcing *Hnrt2.1* to be monophyletic. All highly diverged *nrt2* sequences within a strain were represented by two very similar yet distinct sequences suggesting these were indeed paralogs and not allelic.

Selection

MEC tests of selection (Table 5) found 23 (17 in *Hnrt2.1* only) sites to have a $K_a/K_s > 1$ in *Hebeloma*, which would suggest positive selection, but the lower bound of the confidence interval did not support significance. The Hydnangiaceae alignment had 32 sites with $K_a/K_s > 1$, 12 of these sites had

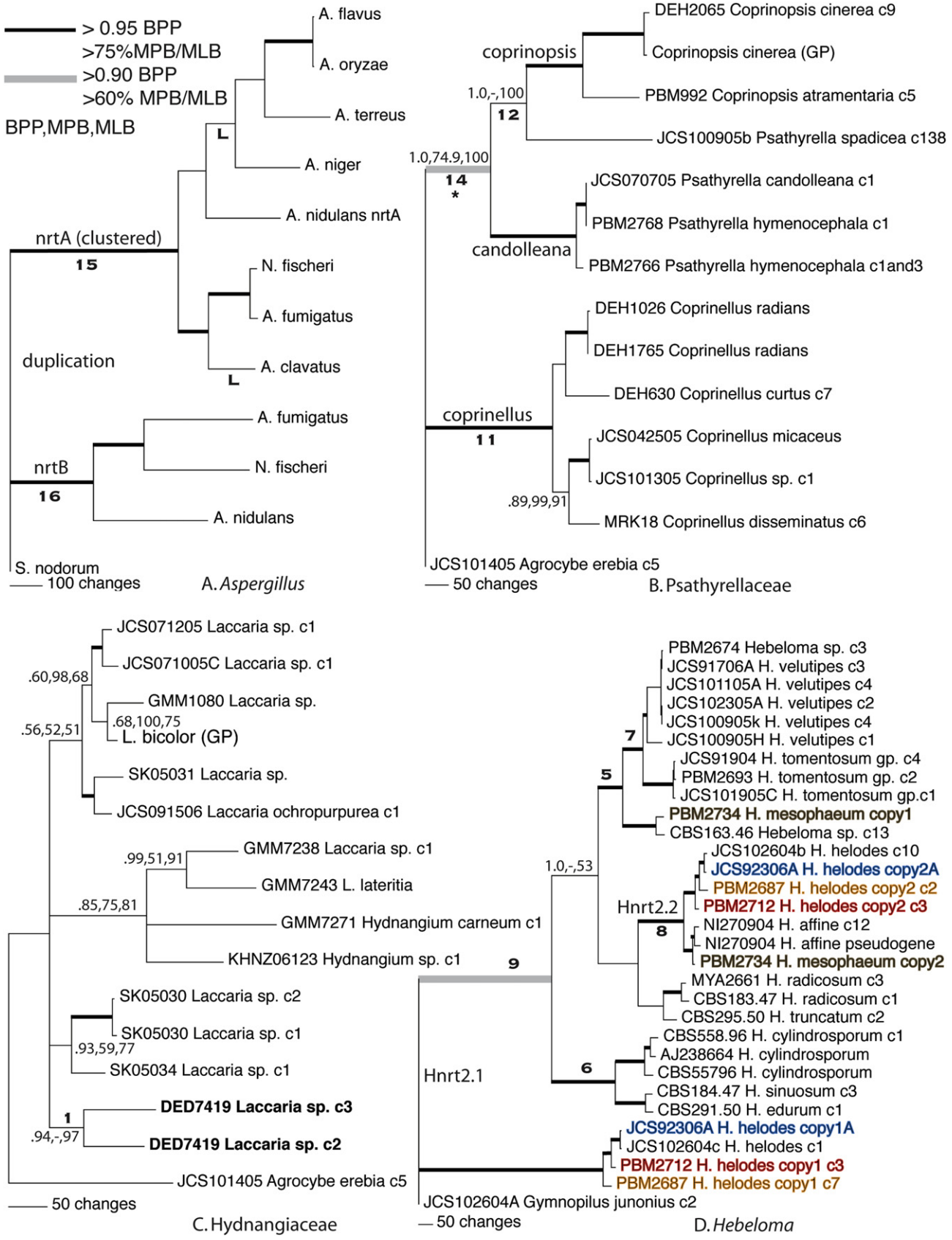

Fig 4 – Phylogenetic analyses of *nrt2* in isolated lineages. Outgroups were chosen from the initial broad analysis (Fig 2). Supported nodes are as in Fig 2. *Aspergillus*, *Hebeloma* and Psathyrellaceae topologies are Maximum Likelihood trees generated in RAxML and the Hydnangiaceae topology is a Bayesian consensus tree. All topologies are optimized with maximum parsimony. Nodes numbered in bold are as in Table 4. Nodes in which *nrtB* is inferred to have been lost assuming the *Aspergillus* topology are noted with a bold "L" in *nrtA* tree. Alternate paralogs of *nrt2* from the same strain have same colored type. The "*" at node 14 indicates conflict with other phylogenies.

Table 4 – Support[a] for select nodes in *nrt2* and ITS phylogenies

Dataset	Node	ITS				*nrt2*			
		BPP	MPB	MLB	Literature[b]	BPP	MPB	MLB	Constraint
Hydnangiaceae	1. DED7419 paralogs	n/a	n/a	n/a		0.94	–	69	–
	2. *Hydnangium/L. lateritia* + DED7419	–	–	–		0.84	–	90	–
	3. DED7419 + *Laccaria* (−*Hydn./L. lat.*)	–	–	–		–	94	–	–
	4. *Laccaria* (−*Hydnangium/L. lateritia*)	–	60	–	Osmundson *et al.* (2005)	–	89	–	–
	5. *H. tomen.* + *H. meso.* + *H. vel. nrt2.1*	–	–	–		0.99	100	96	–
Hebeloma	6. *H. edurum* + *H. cylindrosporum*	100	87.8	99	Aanen *et al.* (2000), Boyle *et al.* (2006)	1.0	96.4	99	–
	7. *H. tomentosum* + *H. velutipes*	–	–	–		1.0	100	100	–
	8. *Hnrt2.2*	n/a	n/a	n/a		1.0	100	100	–
	9. *Hebeloma nrt2* − *H. helodes nrt2.1*	n/a	n/a	n/a		1.0	–	60	–
	10. *Hebeloma nrt2* − *H. helodes nrt2.2*	n/a	n/a	n/a		–	–	–	N.S.[c]
Psathyrellaceae	11. *Coprinellus*	0.93	99.75	63	Padamsee *et al.* (2008)	0.99	99.8	92	–
	12. JCS100905B + *Coprinopsis*	–	–	–		1.0	–	100	–
Aspergillus	13. *Coprinellus* + *Candolleana*	1.0	78.8	100	Padamsee *et al.* (2008)	–	–	–	N.S.
	14. *Coprinopsis* + *Psathyrella spadicea* + *Candolleana*	–	–	–		1.0	74.9	100	
	15. *nrt2A* + clustered	n/a	n/a	n/a		1.0	93	85	–
	16. *nrt2B* − clustered	n/a	n/a	n/a		1.0	73	100	–

a BPP = Bayesian Posterior Probability (>0.95), MPB = Maximum Parsimony Bootstrap % (>50 %), MLB = Maximum Likelihood Bootstrap % (>50 %).
b Previous studies supporting this node.
c $p > 0.05$, SH test implemented in RAxML.

$K_a/K_s > 1.5$, and 6 had confidence intervals that supported significance in at least one model (Table 5). A graphical representation of sites under positive selection is in Fig 5. Only one site in the Psathyrellaceae and two sites in *Aspergillus* had $K_a/K_s > 1$, but neither were supported to be significant. Comparisons of AIC scores supported significantly better fit of the data to the MEC than the M8a null model for all four alignments. The M5 and M8, beta + $\omega \geq 1$ and M5, gamma models inferred 6 and 5 sites respectively to be under significant positive selection and the overall significance of the M8 was $p < 0.001$.

Sequence structure analyses

Results of helical wheel analyses are compared across a phylogeny in Fig 6. Variation was apparent in Tm 2 between copies across lineages despite a background of conservation in Tm helices. Differences in hydrophobicity of the variable amino acid residues in closest spatial proximity to R87 are presented on a phylogeny (Fig 6A). Additionally, we observed coincidental substitution (non-polar to tyrosine) between copy 1 and 2 in *H. helodes* and *H. mesophaeum* in both the homologous sixth and twelfth transmembrane motifs (Fig 6B). Features in the IL regions were also observed to vary between paralogs (Table 6). In particular, putative protein kinase C (PKC) binding motifs of varying levels of conservation across the sample were usually divergent in number between paralogs. The most highly conserved of these motifs were at symmetric ends of the IL, and the one at the N-terminal has apparently experienced convergent substitution to A-D-R in the following lineages (data not shown): *Coprinellus*, *Phanerochaete*, *Postia* (Basidiomycota), and *Tuber*, *Phaeosphaera*, *Aspergillus* and *Stagonospora* (Ascomycota). Most of these sequences with this anomaly were either in wood-decay lineages or known not to occur in a nitrate assimilation gene cluster (excepting *Tuber*, which is thought to be in a cluster).

Relative expression analyses

Cultures of *H. helodes* reached confluence in 12 d in liquid medium. Other *Hebeloma* and *Gymnopilus* cultures reached confluence at different times sooner than 12 d. While *H. helodes* grew in suspension, *H. velutipes* and *H. radicosum* adhered to the Petri plate and *G. junonius* grew at the surface of the medium. In real time RT-PCR expression analyses, inferred PCR efficiencies ranged from 1.84 to 2.06 (Fig 7). Both paralogs of *nrt2* (Fig 7A) were expressed in *H. helodes* cultures exposed to a range of nitrate concentration, but expression levels were highly divergent (>100-fold difference). *Hhnrt2.1*, was highly expressed under nitrate as a sole source of nitrogen and under nitrogen starvation, and repressed by ammonium. *Hhnrt2.2* was not highly expressed under any conditions, yet appeared to display an overall pattern of induction and repression similar to *Hhnrt2.1*. A similar pattern was also observed (Fig 7B) in other *Hebeloma* species and *G. junonius*. Consistent levels of expression were observed within replicates across three nitrate concentrations in the low affinity range. The housekeeping gene *ef1-α*, used to calculate relative expression, was expressed with little variation between experimental treatments compared to large variations in *nrt2* expression. All experiments were replicated at least once on separate occasions with qualitatively similar results, except with *G. junonius* which was conducted successfully only once. While three biological replicates demonstrated the same pattern of divergent expression between *H. helodes* paralogs, absolute values and ratios of expression varied due to experimental limitations. All real time PCR products were of appropriate

Table 5 – Sites[a] with $K_a/K_s > 1.5$[b] in NRT2 in Hydnangiaceae

Site[c]	Location[d]	MEC			M8			M5		
		CI[e]	PP[f]	K_a/K_s	CI	PP	K_a/K_s	CI	PP	K_a/K_s
V250	IL	[0.900838,2.51995]	0.60	1.87165	[0.66,1.9]	0.83	1.7	–	–	–
D255	IL	[0.900838,2.51995]	0.54	1.79297	–	–	–	–	–	–
G259	IL	[1,2.51995]	0.35	1.53202	[1.9,1.9]S[g]	0.99	1.9	[1.6,1.6]S	0.99	1.6
S260	IL	[0.900838,1]	0.94	2.4268	[1.9,1.9]S	0.99	1.9	[1.6,1.6]S	0.99	1.6
R270	IL	[1.77508,3.53291]S	0.99	3.47364	[1.9,1.9]S	0.99	1.9	[1.6,1.6]S	1.0	1.6
K296	IL	[0.439539,2.51995]	0.47	1.66694	[0.43,1.9]	0.76	1.6	–	–	–
L299	IL	[1.19856,3.53291]S	0.98	3.26338	[1.9,1.9]S	0.99	1.9	[1.6,1.6]S	0.99	1.6
N339	E	[1.19856,3.53291]S	0.97	2.90011	[1.9,1.9]S	0.99	1.9	[1.6,1.6]S	0.99	1.6
G370	I	[0.439539,2.51995]	0.51	1.69731	–	–	–	–	–	–
V384	I	[0.900838,1]	0.94	2.43012	[0.66,1.9]	0.96	1.8	[1.6,1.6]S	0.98	1.6
W385	I	[0.900838,1]	0.85	2.27747	[0.66,1.9]	0.91	1.8	[0.68,1.6]	0.94	1.6
H408	E	[0.900838,1]	0.76	2.12882	[0.66,1.9]	0.88	1.7	[0.68,1.6]	0.93	1.6

a Amino acid sites shown in bold received support for significant positive selection from at least one codon substitution model analysis.
b Inferred with Mechanistic Empirical Model (MEC), M8, beta + $\omega \geq 1$ (M8) or M5, gamma (M5) as described in Methods.
c Single letter amino acid abbreviation and position in *Laccaria bicolor* genome sequence.
d Inferred location relative to cell membrane: E = extracellular surface, IL = central large intracellular loop, I = intracellular surface other region.
e Confidence interval between 5th and 95th percentile.
f Bayesian posterior probability.
g Lower bound of confidence interval >1.

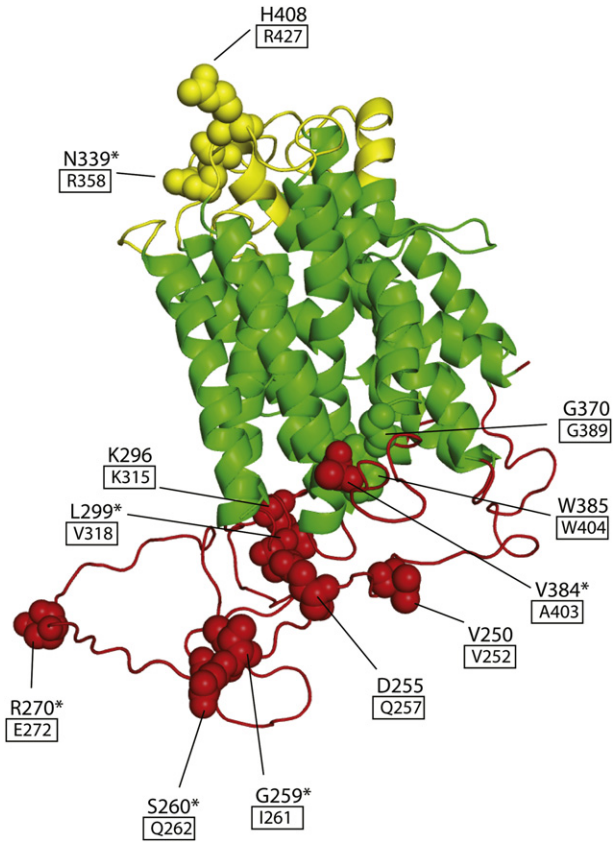

Fig 5 – Three-dimensional rendering of NRT2. Amino acid sites with $K_a/K_s > 1.5$ in Hydnangiaceae are shown with space-filling spheres. Free residue numbers correspond to position in *Laccaria bicolor* genome project NRT2 and boxed residue numbers correspond to the homologous site in *Hebeloma cylindrosporum* (CAB60009). Asterisk denotes sites with lower level of confidence interval >1 for one or more Selecton models described in Methods. Yellow is sequence inferred to be on the extracellular surface, green is sequence inferred to be in the transmembrane region and red is sequence inferred to be in the intracellular surface.

size and dissociation curves for each experiment were determined to contain single products.

Discussion

Our results suggest that duplication of *nrt2* is sporadic in fungi, and has been followed by differential loss (in *Aspergillus* and perhaps *Hebeloma*) and possibly lineage sorting of paralogs. In at least 2 species, *H. helodes* and *A. nidulans* (Unkles *et al.* 2001), these two paralogs are functionally distinct. Unlike the previously characterized paralogs in *Aspergillus*, however, those in *H. helodes* have different levels of expression. A comparison of sequences between paralogs and species from different ecologies suggests sites and motifs to target as potential sites of functional evolution and niche adaptation.

Phylogenetics of nrt2 gene duplication

Previous studies did not detect additional paralogs of *nrt2* in *H. cylindrosporum* (Jargeat *et al.* 2003). We have demonstrated here that in species of at least two mushroom-forming lineages of fungi (*Hebeloma* and Hydnangiaceae) a second form of the gene derived *via* independent duplication events is maintained. Previous work (Nygren *et al.* 2008) and our own unpublished genome project surveys suggest that paralogs of the other constituent genes of the nitrate assimilation cluster are more rare. This is consistent with previous suggestions that duplications in fungi have an elevated frequency in genes encoding transporters and other peripherally active proteins (Wapinski *et al.* 2007).

Duplication of *nrt2* in *Hebeloma* may have occurred early in the diversification of the group, if we accept a basal position of and infer no loss in the *H. cylindrosporum/Hebeloma edurum* clade (Fig 4). This topology is, however, not strongly supported by a variety of phylogenetic methods. Alternatively, the duplication preceded the diversification of *Hebeloma*, but was selectively lost in at least *H. cylindrosporum*. While we failed to detect a second paralog with degenerate PCR in most *Hebeloma* species examined, the phylogenetic distance between the *H. mesophaeum* and *H. helodes* clades suggests that the second paralog could be widespread in this group. Previous surveys of fungal genomes also failed to detect more than two paralogs (Slot *et al.* 2007).

In *Hebeloma*, *nrt2.2* has limited support for being derived from *nrt2.1*, because it is a monophyletic group nested within the other paralog, but this support comes from different topologies inferred by different methods. The *Hnrt2.2* branch is long in a RAxML tree, but divergence between species is less apparent than with *Hnrt2.1*, suggesting a finite period of rapid divergence following duplication. Alternatively, *Hnrt2.1* could be monophyletic. In the latter case, the greater divergence between *nrt2.1* orthologs could suggest adaptation or relaxed selection in *Hnrt2.1*. *Nrt2* was inferred to be under positive selection in *Hebeloma* (discussed below). Results of a constrained analysis forcing the monophyly of *Hnrt2.1* did not, however, have a significantly worse likelihood than the optimal topology.

A second duplication found in *Laccaria* is supported to be restricted to the clade represented by isolate DED7419. It is possible we have failed to detect other paralogs in our sample because our PCR primers might not amplify quickly evolving paralogs. The *Laccaria bicolor* genome reveals no *nrt2* paralogs, confirming that paralogs are not universal in this lineage.

We uncovered no paralogous forms of *nrt2* in Psathyrellaceae. However, the conflict between the phylogenies inferred from rDNA – here and by others (Padamsee *et al.* 2008) – and *nrt2* could suggest a cryptic paralogy that was either sorted out or that we failed to detect. Ribosomal DNA supports a sister relationship between the *Candolleana* and *Coprinellus* clades (Padamsee *et al.* 2008), but *nrt2* results presented here (Fig 5) suggest the *Coprinopsis* clade is nested within a paraphyletic *Psathyrella* clade. Alternatively, the result could reflect an inappropriate rooting with *A. erebia*, as the larger *nrt2* alignment supports the rDNA phylogeny. Some

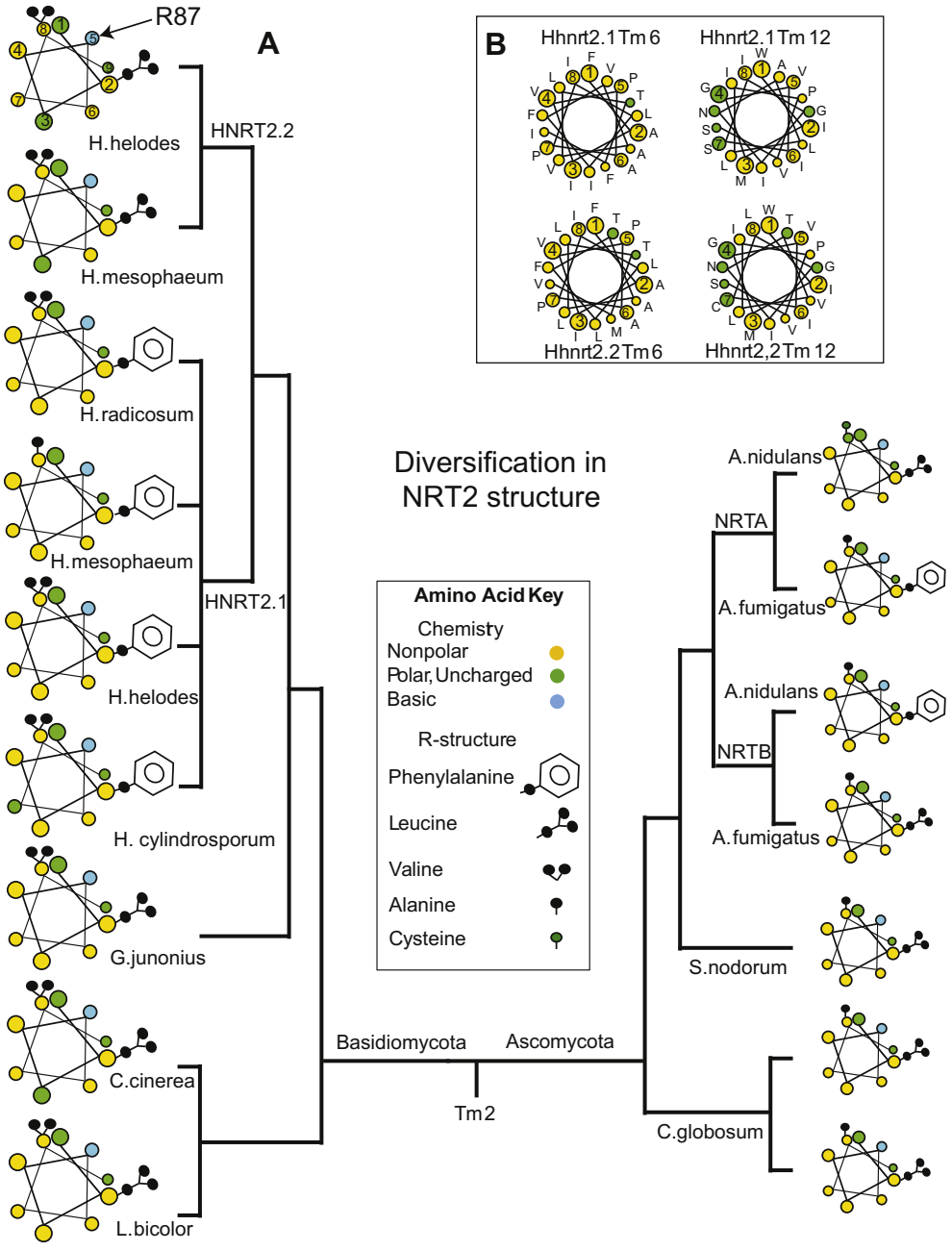

Fig 6 – Comparison of structural motifs in NRT2 sequences. (A) Helical wheel analysis of the nine C-terminal residues of transmembrane helix # 2 with the highly variable nearest non-polar residues accentuated by R-group structure. These sites diverge similarly between paralogs in *Hebeloma* and *Aspergillus* (fumigatus and nidulans). Stagonospora nodorum and Chaetomium globosum are included as outgroups. The phylogeny agrees with that in Fig 3 (for Basidiomycota) and Fig 4 (for Ascomycota). Phylogenetic placement of *C. globosum* is as in Slot *et al.* (2007). (B) Comparison of eighteen amino acids of transmembrane helix #s 6 and 12 between *nrt2* paralogs in *H. helodes*.

support for the restricted *nrt2* topology comes from a shared feature between *Candolleana* and *Coprinopsis* sequences, which may have functional significance. The highly conserved protein kinase C motif near the N-terminus of the large intracellular loop is lacking in *Coprinellus* and the nearest outgroup of Psathyrellaceae in this dataset, *A. erebia*. The potential functional significance of this motif could suggest *Coprinopsis* and *Psathyrella/Candolleana nrt2* are derived from a common paralog that diverged and adapted early in the evolution of Psathyrellaceae. More likely, the similarities between *Coprinopsis* and *Psathyrella/Candolleana* primary structure could represent functional convergence on a favored motif or common mutation that has occurred in multiple lineages, or the *Coprinellus* feature could be derived. While paralogous forms of *nrt2* were not found in Psathyrellaceae (or in the *Coprinopsis cinerea* genome), successful PCR amplification was also limited to one primer pair, which could have favored a single paralog.

Table 6 – Comparison of structural properties of *nrt2* paralogs and orthologs in fungi

	Paralog[a] 1					Paralog 2				
	Clustering/ Presence[b]	#PKC[c] (in IL)	Length IL[d]	Putative binding site[e]	#C 84+90 (N,C)[f]	Clustering /Presence	#PKC (in IL)	Length IL	putative binding site	#C 84+90
H.helodes	P-C	8(6)	90	TFVVRIMVG	10(7,3)	P-NC	2(2)	87	TLGMRVIVG	7(4,3) OG[g]
H. cylindrosporum	S-C	9(6)	91	TFVVRVGVG	10(7,3)	A				
H.mesophaeum	?	?(3)	89	TFVVRVVAG	8(7,1)	?	?(4)	88	TLGIRIIVG	7(4,3) OG
H. affine	U	?	?	?	?	?	?(1)	87	?	?
H. velutipes[h]	?	?(4)	90	TFVVRIVAG	8(7,1)	U	?	?	?	?
H. radicosum[i]	?	?(4)	88	TFFVRAAVG	10(7,3)	U	?	?	?	?
L. sp. DED7419	?	?(3)	73	?	?	?	?(1)	70	?	?
L.bicolor	G-C	4(2)	73	TLAVRLFVG	7(4,3)	A				
A.nidulans	G-C	6(4)	93	TLLVRLICG	4 + S[j] (4,S)	G-NC	5(2)	82	TFVMRFIAG	8(7,1)
Aspergillus fumigatus	G-C	10(5)	92	TFLVRFIAG	8(7,1)	G-NC	6(4)	85	TLLMRFIAG	5(4,1)
Neosartorya fischeri	G-C	10(5)	92	TFLVRFIAG	8(7,1)	G-NC	5(3)	85	TLLMRFIAG	5(4,1)
C.globosum	G-NC	?(1)	99	TLLVRVVAG	5(4,1)	G-NC	?(0)	100	TLAVRVVAG	5(4,1)
C. cinerea	G-C	2(2)	88	TLGVRFAVG	7(4,3) OG	A				
Stagonospora nodorum	G-NC	?(1)	90	TLIVRFIAG	5(4,1)	A				
G. junonius	?	?(3)	83	TLVLRILVG	7(4,3)	U	?	?	?	?

[a] Paralogs in dark grey-filled cells were expressed in this study, in black are confirmed not to exist and light grey not confirmed to exist.
[b] P-C = Putatively clustered (with nitrate reductase and nitrite reductase genes). S-C = Clustering is confirmed by sequencing. G-C = Clustering is confirmed by genome project. P-NC and G-NC = clustering putative or confirmed by genome project. U = Presence in genome unknown. A = absence confirmed.
[c] The number of Protein Kinase C binding motifs in the entire sequence, if known or (in the large intracellular loop-IL-only).
[d] The number of amino acid sites inferred to make up the IL
[e] Residues in bold diverge between paralogs and are displayed in fig. 7.
[f] The number of carbon atoms in R-groups as a measure of hydrophobicity in the nearest variable hydrophobic residues to conserved residue R87 in Tm helix 2, (in the N most residue, and the C-most residue).
[g] Glycine residue on hydrophobic side of Tm helix 2.
[h] Sequence data derived from CBS163.47 and expression data from JCS91706A.
[i] Strain MYA2661.
[j] Cysteine residue instead of hydrophobic residue.

In both Hydnangiaceae and Psathyrellaceae, the placement of the genome project sequences agreed with an organismal phylogeny for the group (*L. bicolor* genome *nrt2* is sister to *nrt2* from species that are phylogenetically close to *L. bicolor* isolates according to ITS sequences in GenBank, and the *C. cinerea* genome *nrt2* is sister to DEH2065, identified as *C. cinerea* by Don Hemmes (University of Hawai'I, Hilo)). This is important because in both the *L. bicolor* and *C. cinerea* genomes, the single *nrt2* sequence is clustered, suggesting that we likely amplified the clustered or ancestrally clustered paralog in these lineages in the case of any cryptic paralogy (see below, Gene clustering).

Gene clustering

An analysis of *nrt2* in seven complete *Aspergillus* genomes provides a broader context for comparison of independently derived paralogs in *Aspergillus* and *Hebeloma*. We found that clustering with nitrate and nitrite reductase genes is the exclusive property of *nrtA*, with a single duplication event leading to the unclustered *nrtB*. The unclustered *nrtB* is not retained in five of eight lineages, which retain *nrtA*, representing at least two losses (in *Aspergillus clavatus* and an unsupported lineage containing *Aspergillus flavus*, *Aspergillus oryzae*, *Aspergillus terreus*, and *Aspergillus niger*) of the unclustered paralog. There is no species in those examined that possesses *nrtB* without *nrtA*. The only other fungal genome known to contain paralogs of *nrt2*, *Chaetomium globosum* (Slot *et al.* 2007), contains only unclustered sequences. This species also belongs to Sordariomycetes, which has received the nitrate assimilation cluster by horizontal gene transfer in one lineage (Slot & Hibbett 2007). The *Aspergillus* data support conclusions reached recently (Wapinski *et al.* 2007) that duplicate modules are uncommon in fungi, and that the fate of duplicate genes is generally loss. It could also support the ''selfish cluster'' hypothesis (Walton 2000), which predicts improved fitness of genes maintained in functionally related clusters. The only specimen in our dataset that might have undergone alternative sorting (to maintain only *Hnrt2.2*) is *H. affine*, but we have no strong evidence that this is the case, so *nrt2.1* at this point appears to be the more highly retained paralog. We could thus hypothesize that *Hnrt2.2* is a non-clustered paralog, judging by its apparently restricted distribution, apparently derived status, and differences with the *H. cylindrosporum nrt2*, which is known to be clustered. This could account for its divergent pattern of expression relative to the other paralog and other species.

Sequence structure analyses

Structural differences in *nrt2* from different species could reflect adaptation, and regions conserved among paralogs

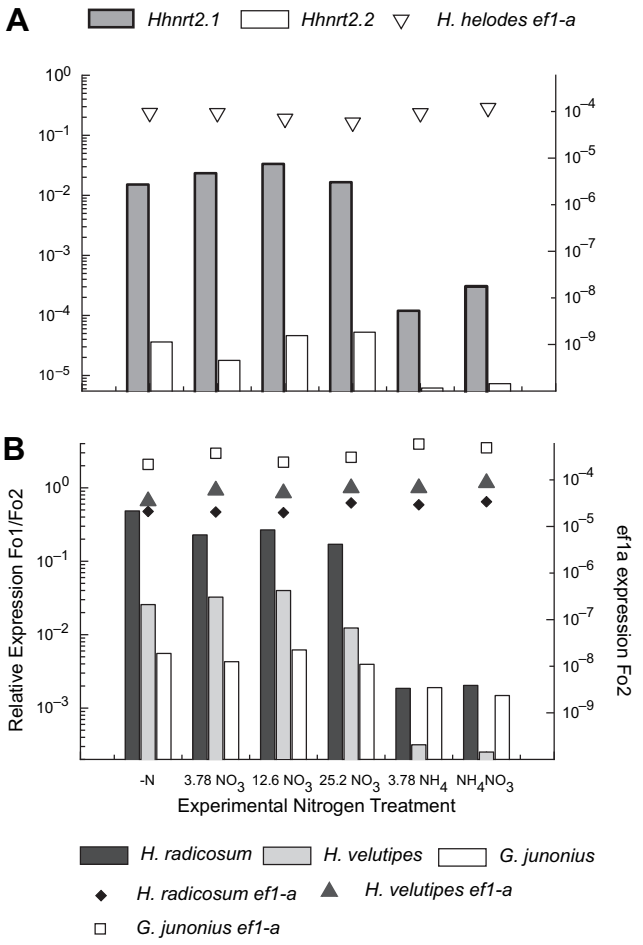

Fig 7 – Real time RT-PCR expression of *nrt2* transcript. (A) Relative transcript abundance of *Hhnrt2.1* and *Hhnrt2.2* (Y-1, left) and hypothetical initial template of the housekeeping gene *ef1-α* (Y-2, right) after 24 hr on noted sole nitrogen source. (B) Relative transcript abundance of *nr2.1* in three related species of mushroom-forming fungi. Axes are as in A. Concentrations are in mM total N, and ammonium nitrate-N is 3.78 mM. F_o1/F_o2 is the ratio of gene of interest to housekeeping gene theoretical initial fluorescence.

may indicate subtle differences in their relative functions (Li & Gallin 2005; Jackson *et al.* 2007). Table 6 compares structural differences between paralogs in different strains of fungi that could be subjected to future mutation and chimera analyses in order to better understand the physiology of transporter diversification (Stieber *et al.* 2003). A discussion of features follows.

Transmembrane helix 2 has an N-terminus outside and C-terminus inside the cell according to helical motif prediction software (Jargeat *et al.* 2003; Slot *et al.* 2007). It has a variable region around R87 (toward the cytoplasm), a putative substrate-binding site, which is nested in a largely hydrophobic region. It was previously shown that replacement of R87 with a lysine residue decreased the substrate affinity of the transporter by at least two orders of magnitude (Unkles *et al.* 2004). Such a replacement has not been observed, so it is likely not a natural means of evolving a higher capacity for nitrate transport. However, the degree of hydrophobicity nearest R87 (according to helical wheel analysis, Fig 6A) varies with respect to two main residues in *A. nidulans* (positions 84 and 90), and the differences are coincident with only a 10-fold divergence in substrate affinity in *A. nidulans*. Paralogs in the lineages in this study tend to diverge in the degree of hydrophobicity afforded by these two residues (Table 6), which could influence the degree to which the helix is embedded in the lipid layer of the membrane. There is also variation in the balance of hydrophobicity between the two (Fig 6A), which could introduce differential torque on the helix. Additionally, helices also may vary with respect to a glycine residue in the hydrophobic region opposite R87, a feature that distinguishes two lineages of *Hebeloma* paralogs. We speculate that these differences tend to introduce variation in level of exposure of R87 and/or pore size in NRT2, thereby influencing the substrate affinity or capacity of the transporter. Interestingly, the mirror-image Tm 8 which contains the homologous R368 exhibits far less variability in the two corresponding nearest varying neighbors, usually with even minor substitutions (e.g. L → I) happening between genera as opposed to between species and paralogs as seen in Tm 2. This region of Tm 8 is more hydrophilic, and so may be less embedded in the lipid bilayer, forming more of the pore structure than the same region of the homologous Tm 2. It is worth noting that positions corresponding to 89 and 90 were shown to have $K_a/K_s > 1$ in *Hebeloma*, and could be directly or secondarily related to differential function in this region. This region was not amplified in *Laccaria* paralogs, where positive selection was better supported. The variability of hydrophobic residues two and three sites upstream and downstream of the highly conserved R87 is reminiscent of the VKC (potassium channel) transporter family. There several sites two positions removed from highly conserved acidic residues in Tm helices had similar variability in non-polar amino acids, and were inferred to be among the most highly informative sites for predicting voltage modulation (Li & Gallin 2005).

Another transmembrane feature that diverges between paralogs in multiple parts of the NRT2 phylogeny is the twelfth position in Tm 6 and Tm 12 (Fig 6B). Derived (or putatively derived) paralogs in both *Hebeloma* and *Aspergillus* have experienced substitution of the non-polar residue at this position in Tm 12, and in *Hebeloma*, the homologous position in Tm 6 has the same substitution (to tyrosine). It is difficult to assign exact homology between *Aspergillus* and *Hebeloma* Tm 6 residues due to differential length in this region.

Another structural variable, which is currently under investigation elsewhere, concerns putative post-translational modification sites in the large intracellular loop. One group found that in *H. polymorpha YNT1* (an *nrt2* homolog) ubiquitin-mediated degradation of the transporter requires a ''PEST-like'' sequence in the IL (Navarro *et al.* 2006). The PESTfind algorithm predicts a differential number of ''poor'' PEST sequences between the N-terminus and IL of paralogs in our dataset (fewer in the derived paralog, data not shown). Another group has found evidence of post-translational down-regulation of NRTA in *A. nidulans* (Wang *et al.* 2007), and is currently investigating the effects of mutating potential phosphorylation sites in order to find a mechanism for this

post-translational regulation. These motifs are potentially interesting for investigations of functional divergence. For instance, Chl1, a nitrate transporter from a different gene family in *Arabidopsis* functions with dual-affinity; high when phosphorylated, low when not (Liu & Tsay 2003). Our analyses suggest that paralogous transporters tend to diverge in the number of at least one class of phosphorylation motif, with deletions and substitutions apparent that would eliminate specific potential PKC recognition sites. With respect to one of these motifs (the STK at the N-terminus of the IL noted previously (Jargeat *et al.* 2003)), we can even observe convergent duplicate point mutations that change the S-x-R to A-D-R in multiple lineages, possibly suggesting a selected trait. In addition to differences in potential PEST and phosphorylation motifs, we see a general reduction in size of the IL in secondary copies. It is plausible that certain regulatory features are selectively modified after gene duplication, which contribute to novel or complementary functions of preserved paralogs. The IL in *Hebeloma* contains eight sites with $K_a/K_s > 1$ (Table 5) and Hydnangiaceae contains fifteen, with several under significant positive selection, suggesting this is an active site of molecular evolution.

The taxon that partly defies a trend of divergence suggested above is *H. mesophaeum*, which has mixed characteristics in its paralogs. It is worth noting that this is also the only *Hebeloma* for which two paralogous *nrt2* sequences were obtained using a single primer pair, and that two primer pairs amplified both paralogs. This, along with the lesser structural differentiation could suggest the *H. mesophaeum* paralogs are not experiencing the same level of functional divergence, so it would be interesting to compare the relative expression profile of this species to that of *H. helodes*.

Functional diversification

Through real time RT-PCR expression analyses, we determined that both paralogs of *nrt2* in *H. helodes* are expressed. Similar levels of expression across a range of low affinity nitrate concentrations suggest that the induction response was saturated. *Hhnrt2.1* is expressed at a much higher level than *Hhnrt2.2* under identical conditions, but both show a common pattern: elevated expression under nitrogen starvation and nitrate as a sole source of nitrogen, and repressed expression in ammonium. There could be several explanations for the divergence. *Hhnrt2.2* could be expressed more highly under a higher affinity/lower capacity range of nitrate concentration (<1 mM), which we did not test, but repressed under the high nitrate conditions we tested. Alternatively, *Hhnrt2.2* might only be expressed in low concentrations. The similarity between expression profiles suggests either a shared or similar regulatory pathway, but it is also possible that one paralog responds to nitrate influx managed by the other.

The exact role of *Hhnrt2.2* is not known, although the generation of truly novel functions through gene duplication has been shown to be rare in fungi (Wapinski *et al.* 2007). The NRT2 family in plants is, however, replete with examples of neo-functionalization (Chopin *et al.* 2007). Perhaps *nrt2* paralogs perform alternative functions in basidiomycetes as well. For comparison, it has been suggested that fungal high affinity ammonium transporters are involved in ''nitrogen sensing'' (Javelle *et al.* 2003), to signal change in growth patterns. Secondary copies could even serve as nitrate exporters to mycorrhizal plants.

We initially expected to observe divergence in the pattern of expression between lineages in different niches. In fact we found similar patterns, but different levels and fold-changes of expression. For instance, the nitrogen-loving, ectomycorrhizal *H. radicosum* exhibited the highest level of expression at 24 hr, and the wood-saprotroph, *G. junonius* the lowest. Differences in expression could be a result of differential rates or volumes of message accumulation. A direct comparison of amount of expression between species is also difficult because of different growth strategies. For example, we had to treat *H. radicosum* earlier because adhesion to the growth chamber hastened crowding of hyphae. We observed differences in ultimate expression level between replicates treated at slightly different stages of hyphal growth, but not in the overall pattern. Also, oxygen access could vary between species because of differential depth, density and activity of mycelia in the media. Differential feedback from substrate and products could also have a confounding effect. Some, but not all of these issues could be largely resolved with different methods and by time curves of expression, but are beyond the scope of our current study, which merely sought to establish evidence of functional divergence.

Our results contrast with the only other expression analysis of paralogous fungal *nrt2* in *A. nidulans* in which identical expression of *nrtA* and *nrtB* led to the conclusion of partial ''genetic redundancy'' with respect to nitrate uptake (Unkles *et al.* 2001). Instead, we have demonstrated that *H. helodes* expresses paralogs of *nrt2* differently. The discrepancy between these species could reflect differences in the environments where each is found. It could also reflect a more streamlined regulatory apparatus in *A. nidulans*, although there is no evidence that the *A. nidulans* genome is smaller than the *H. helodes* genome. It is puzzling that *A. nidulans* should maintain identical regulation between the paralogs when one paralog is located in a gene cluster containing specific regulatory elements and the other is dispersed. The case of *H. helodes*, where expression has diverged, is less surprising. Finally, in *A. nidulans*, the derived paralog (*nrtB*) codes for a higher affinity transporter (K_m 10 μM *versus* 100 μM). As there was no strong expression response in the lower affinity range with *Hhnrt2.2* it is possible that the putatively derived copy in *H. helodes* codes for a strictly high affinity transporter, which would require a nitrate concentration-dependent repression mechanism. It is also possible that *nrtB* in *A. nidulans* would be down-regulated at concentrations greater than 5 mM, which were the range of concentrations used in this study, but not previously explored with *A. nidulans*.

Differential evolution and selection in nrt2 between mushroom-forming lineages with different ecologies

Any comparisons between the *nrt2* phylogenies from contrasting lineages presented here would likely be influenced by

organismal phylogeny, which is not highly resolved for *Hebeloma* or Hydnangiaceae. A test of positive selection may have detected differences in the role of nitrate acquisition in these lineages. We found approximately 40 % more sites with a $K_a/K_s > 1$ in Hydnangiaceae (32 sites) compared to *Hebeloma* (23 sites). By contrast, we only found a single site with $K_a/K_s > 1$ in the IL of the Psathyrellaceae alignment. Hydnangiaceae was the only lineage with amino acid sites (6) under significant positive selection. The results could reflect the relative levels of divergence in the clades, as synonymous substitutions should eventually overwhelm temporary elevations in non-synonymous substitutions (Zhang *et al.* 2005). However, the results might also reflect increased positive selection on the mycorrhizal lineages. This could be explained by the extensive host-switching these lineages have undergone that could change both the overall demand for nitrogen and the environmental accessibility of nitrate. Purifying selection is predictably strongest in transmembrane helices where structural integrity and hydrophobicity are crucial to function, and in functionally essential residues and signature sequences. The overall *nrt2* alignment was under significant positive selection in all lineages tested, regardless of whether specific sites were found to be under significant positive selection.

Regarding differences in gene duplication events, it appears that the paralogs we uncovered in *Hebeloma* and *Laccaria* have been diverging for different portions of the evolution of the genera. The *Hebeloma* duplication happened early in the lineage judging by the phylogenetic distance between taxa possessing both *nrt2.1* and *nrt2.2*, while the *Laccaria* duplication happened more recently in Hydnangiaceae diversification. We cannot rule out additional paralogs in Hydnangiaceae, although the *L. bicolor* complete genome suggests paralogy is not universal in Hydnangiaceae. The same is true for Psathyrellaceae and the *C. cinerea* genome where duplication also appears restricted.

A comparison of the structural details we chose to focus on in this study reveals some lineage-specific characteristics. First, *Hebeloma* has a paralog, *Hnrt2.1*, with the highest number of potential PKC binding motifs in the IL (4-7). Hydnangiaceae and Psathyrellaceae IL, for which data are not shown, usually have one to three motifs like the selection shown in Table 6. *Hnrt2.2* has a PKC motif number more similar to Hydnangiaceae and Psathyrellaceae ILs. *Hebeloma* also has longer ILs on average than the other lineages, although *Hnrt2.2* IL is similar in length to that of Psathyrellaceae. A comparison of the potential binding site (near R87) diversity was limited by the short sequences we generated in Hydnangiaceae and Psathyrellaceae, but the sites in the genome project sequences tend to agree with the IL data, which suggests these lineages are more similar to *Hnrt2.2*.

Acknowledgements

We would like to thank Nancy Ironside for kindly providing material, and Camilo Khatchikian for thoughtful discussions and for writing the STK counting code mentioned in the methods. Thanks also to Andy Taylor for thoughtful exchanges. This work was supported by the National Science Foundation Doctoral Dissertation Improvement Grant DEB-0608017.

Supplementary material

Supplementary data associated with this article can be found in the online version at doi:10.1016/j.funeco.2009.10.001.

REFERENCES

Aanen DK, Kuyper TW, Hoekstra RF, 2000. Phylogenetic relationships in the genus *Hebeloma* based on ITS1 and 2 sequences, with special emphasis on the *Hebeloma crustuliniforme* complex. *Mycologia* **92**: 269–281.

Altekar G, Dwarkadas S, Huelsenbeck JP, Ronquist F, 2004. Parallel Metropolis coupled Markov chain Monte Carlo for Bayesian phylogenetic inference. *Bioinformatics* **20**: 407–415.

Batsch A, Noetel A, Fork C, Urban A, Lazic D, Lucas T, Pietsch J, Lazar A, Schomig E, Grundemann D, 2008. Simultaneous fitting of real-time PCR data with efficiency of amplification modeled as Gaussian function of target fluorescence. *BMC Bioinformatics* **9**: 95.

Boyle H, Zidmars B, Renker C, Buscot F, 2006. A molecular phylogeny of Hebeloma species from Europe. *Mycological Research* **110**: 369–380.

Brito N, Avila J, Perez MD, Gonzalez C, Siverio JM, 1996. The genes YNI1 and YNR1, encoding nitrite reductase and nitrate reductase respectively in the yeast *Hansenula polymorpha*, are clustered and co-ordinately regulated. *Biochemical Journal* **317**: 89–95.

Chopin F, Orsel M, Dorbe MF, Chardon F, Truong HN, Miller AJ, Krapp A, Daniel-Vedele F, 2007. The Arabidopsis ATNRT2.7 nitrate transporter controls nitrate content in seeds. *Plant Cell* **19**: 1590–1602.

Doron-Faigenboim A, Pupko T, 2007. A combined empirical and mechanistic codon model. *Molecular Biology and Evolution* **24**: 388–397.

Doron-Faigenboim A, Stern A, Mayrose I, Bacharach E, Pupko T, 2005. Selecton: a server for detecting evolutionary forces at a single amino-acid site. *Bioinformatics* **21**: 2101–2103.

Gardes M, Bruns TD, 1993. ITS primers with enhanced specificity for basidiomycetes – application to the identification of mycorrhizae and rusts. *Molecular Ecology* **2**: 113–118.

Jackson HA, Marshall CR, Accili EA, 2007. Evolution and structural diversification of hyperpolarization-activated cyclic nucleotide-gated channel genes. *Physiological Genomics* **29**: 231–245.

Jargeat P, Rekangalt D, Verner MC, Gay G, Debaud JC, Marmeisse R, Fraissinet-Tachet L, 2003. Characterisation and expression analysis of a nitrate transporter and nitrite reductase genes, two members of a gene cluster for nitrate assimilation from the symbiotic basidiomycete *Hebeloma cylindrosporum*. *Current Genetics* **43**: 199–205.

Javelle A, Andre B, Marini AM, Chalot M, 2003. High-affinity ammonium transporters and nitrogen sensing in mycorrhizas. *Trends in Microbiology* **11**: 53–55.

Johnstone IL, McCabe PC, Greaves P, Gurr SJ, Cole GE, Brow MA, Unkles SE, Clutterbuck AJ, Kinghorn JR, Innis MA, 1990. Isolation and characterisation of the crnA-niiA-niaD gene cluster for nitrate assimilation in *Aspergillus nidulans*. *Gene* **90**: 181–192.

Katoh K, Toh H, 2008. Recent developments in the MAFFT multiple sequence alignment program. *Briefings in Bioinformatics* **9**: 286–298.

Li B, Gallin WJ, 2005. Computational identification of residues that modulate voltage sensitivity of voltage-gated potassium channels. *BMC Structural Biology* **5**: 16.

Liu KH, Tsay YF, 2003. Switching between the two action modes of the dual-affinity nitrate transporter CHL1 by phosphorylation. *The Embo Journal* **22**: 1005–1013.

Maddison WP, Maddison DR, 2000. *MacClade 4: Analysis of Phylogeny and Character Evolution*. Sinauer Associates, Sunderland, MA.

Matheny PB, Curtis JM, Hofstetter V, Aime MC, Moncalvo JM, Ge ZW, Slot JC, Ammirati JF, Baroni TJ, Bougher NL, Hughes KW, Lodge DJ, Kerrigan RW, Seidl MT, Aanen DK, DeNitis M, Daniele GM, Desjardin DE, Kropp BR, Norvell LL, Parker A, Vellinga EC, Vilgalys R, Hibbett DS, 2006. Major clades of Agaricales: a multilocus phylogenetic overview. *Mycologia* **98**: 982–995.

Montanini B, Viscomi AR, Bolchi A, Martin Y, Siverio JM, Balestrini R, Bonfante P, Ottonello S, 2006. Functional properties and differential mode of regulation of the nitrate transporter from a plant symbiotic ascomycete. *Biochemical Journal* **394**: 125–134.

Navarro FJ, Machin F, Martin Y, Siverio JM, 2006. Down-regulation of eukaryotic nitrate transporter by nitrogen-dependent ubiquitinylation. *Journal of Biological Chemistry* **281**: 13268–13274.

Nygren CM, Eberhardt U, Karlsson M, Parrent JL, Lindahl BD, Taylor AF, 2008. Growth on nitrate and occurrence of nitrate reductase-encoding genes in a phylogenetically diverse range of ectomycorrhizal fungi. *New Phytologist* **180**: 875–889.

Orsel M, Krapp A, Daniel-Vedele F, 2002. Analysis of the NRT2 nitrate transporter family in Arabidopsis. Structure and gene expression. *Plant Physiology* **129**: 886–896.

Osmundson TW, Cripps CL, Mueller GM, 2005. Morphological and molecular systematics of Rocky Mountain alpine Laccaria. *Mycologia* **97**: 949–972.

Padamsee M, Matheny PB, Dentinger BT, McLaughlin DJ, 2008. The mushroom family Psathyrellaceae: evidence for large-scale polyphyly of the genus *Psathyrella*. *Molecular Phylogenetics and Evolution* **46**: 415–429.

Peirson SN, Butler JN, Foster RG, 2003. Experimental validation of novel and conventional approaches to quantitative real-time PCR data analysis. *Nucleic Acids Research* **31**: e73.

Porollo A, Meller J, 2007. Versatile annotation and publication quality visualization of protein complexes using POLYVIEW-3D. *BMC Bioinformatics* **8**: 316.

Porollo AA, Adamczak R, Meller J, 2004. POLYVIEW: a flexible visualization tool for structural and functional annotations of proteins. *Bioinformatics* **20**: 2460–2462.

Rechsteiner M, Rogers SW, 1996. PEST sequences and regulation by proteolysis. *Trends in Biochemical Sciences* **21**: 267–271.

Rogers S, Wells R, Rechsteiner M, 1986. Amino acid sequences common to rapidly degraded proteins: the PEST hypothesis. *Science* **234**: 364–368.

Ronquist F, Huelsenbeck JP, 2003. MrBayes 3: Bayesian phylogenetic inference under mixed models. *Bioinformatics* **19**: 1572–1574.

Slot JC, Hallstrom KN, Matheny PB, Hibbett DS, 2007. Diversification of NRT2 and the origin of its fungal homolog. *Molecular Biology and Evolution* **24**: 1731–1743.

Slot JC, Hibbett DS, 2007. Horizontal transfer of a nitrate assimilation gene cluster and ecological transitions in fungi: a phylogenetic study. *PLoS ONE* **2**: e1097.

Stamatakis A, 2006. RAxML-VI-HPC: maximum likelihood-based phylogenetic analyses with thousands of taxa and mixed models. *Bioinformatics* **22**: 2688–2690.

Stern A, Doron-Faigenboim A, Erez E, Martz E, Bacharach E, Pupko T, 2007. Selecton 2007: advanced models for detecting positive and purifying selection using a Bayesian inference approach. *Nucleic Acids Research* **35**: W506–W511.

Stieber J, Thomer A, Much B, Schneider A, Biel M, Hofmann F, 2003. Molecular basis for the different activation kinetics of the pacemaker channels HCN2 and HCN4. *Journal of Biological Chemistry* **278**: 33672–33680.

Swofford DL, 2003. *PAUP*. Phylogenetic Analysis Using Parsimony (*and Other Methods). Version 4*. Sinauer Associates, Sunderland, Massachusetts.

Unkles SE, Hawker KL, Grieve C, Campbell EI, Montague P, Kinghorn JR, 1991. crnA encodes a nitrate transporter in *Aspergillus nidulans*. *Proceedings of the National Academy of Sciences of the United States of America* **88**: 204–208.

Unkles SE, Rouch DA, Wang Y, Siddiqi MY, Glass AD, Kinghorn JR, 2004. Two perfectly conserved arginine residues are required for substrate binding in a high-affinity nitrate transporter. *Proceedings of the National Academy of Sciences of the United States of America* **101**: 17549–17554.

Unkles SE, Zhou D, Siddiqi MY, Kinghorn JR, Glass AD, 2001. Apparent genetic redundancy facilitates ecological plasticity for nitrate transport. *The EMBO Journal* **20**: 6246–6255.

Walton JD, 2000. Horizontal gene transfer and the evolution of secondary metabolite gene clusters in fungi: an hypothesis. *Fungal Genetics and Biology* **30**: 167–171.

Wang Y, Li W, Siddiqi Y, Kinghorn JR, Unkles SE, Glass AD, 2007. Evidence for post-translational regulation of *NrtA*, the *Aspergillus nidulans* high-affinity nitrate transporter. *New Phytologist* **175**: 699–706.

Wapinski I, Pfeffer A, Friedman N, Regev A, 2007. Natural history and evolutionary principles of gene duplication in fungi. *Nature* **449**: 54–61.

Zhang J, Nielsen R, Yang Z, 2005. Evaluation of an improved branch-site likelihood method for detecting positive selection at the molecular level. *Molecular Biology and Evolution* **22**: 2472–2479.

Zhou JJ, Trueman LJ, Boorer KJ, Theodoulou FL, Forde BG, Miller AJ, 2000. A high affinity fungal nitrate carrier with two transport mechanisms. *Journal of Biological Chemistry* **275**: 39894–39899.